Clinical Radiology 78 (2023) 601–607

Contents lists available at ScienceDirect

Clinical Radiology

journal homepage: www.clinicalradiologyonline.net

Brain iron deposition is positively correlated with cognitive impairment in patients with chronic cerebral hypoperfusion: a MRI susceptibility mapping study

J.-J. Yu [a,†], C. Li [b,†], Z.-M. Qian [c,*], Y. Liu [a,**]

[a] *Department of Pain and Rehabilitation, The Second Affiliated (Xinqiao) Hospital, The Army (Third Military) Medical University, Chongqing 400038, China*
[b] *Department of Medical Imaging, Chongqing University Central Hospital, Chongqing, China*
[c] *Institute of Translational & Precision Medicine, Nantong University, 19 Qi Xiu Road, Nantong, JS 226019, China*

ARTICLE INFORMATION

Article history:
Received 18 July 2022
Received in revised form
14 February 2023
Accepted 27 February 2023

AIM: To investigate the relationship of brain iron deposition with cognitive impairment in patients with chronic cerebral hypoperfusion (CHP).

MATERIALS AND METHODS: Brain iron deposition was detected using quantitative susceptibility mapping (QSM), and cognitive function by neuropsychological tests including the Mini Mental State Examination (MMSE), Montreal Cognitive Assessment (MoCA), Activities of Daily Living (ADLs), and verbal fluency tests in a total of 40 participants, 23 with CHP and 17 age- and sex-matched healthy participants without CHP (controls).

RESULTS: The neuropsychological tests revealed that cognitive impairment ($p<0.05$) and susceptibility values ($p<0.05$) of the bilateral hippocampus (HP) and substantia nigra (SN) in CHP patients were significantly higher than those of the controls. The susceptibility values of bilateral HP and left putamen correlated closely with the scores of neuropsychological tests in the CHP patients ($p<0.05$, $r^2>0.1$). The susceptibility values in the left putamen and bilateral HP were significantly higher in CHP patients with mild cognitive impairment (MCI; $n=8$) than those of CHP patients without MCI ($n=15$; $p<0.05$).

CONCLUSIONS: The present findings indicated that brain iron deposition in specific areas may be responsible for the cognitive impairment in CHP patients, and that QSM is a useful tool to determine brain iron, predicting cognitive impairment in CHP patients.

* Guarantor and correspondent: Z.-M. Qian, Institute of Translational & Precision Medicine, Nantong University, Nantong, JS 226019. China.
** Guarantor and correspondent: Y. Liu, Department of Pain and Rehabilitation, The Second Affiliated (Xinqiao) Hospital, The Army (Third Military) Medical University, Chongqing 400038, China.
E-mail addresses: zhongmingqian2022@163.com (Z.-M. Qian), liuyongd3jydx@sina.com (Y. Liu).
† These authors are first co-authors.

https://doi.org/10.1016/j.crad.2023.02.020
0009-9260/

Introduction

Chronic cerebral hypoperfusion (CHP), induced by long-standing hypertension or severe carotid stenosis, can lead to ischaemic white matter injury resulting in vascular dementia,[1] which is one of the most common forms of dementia in the elderly.[2] Clinically, most cases of CHP are difficult to identify at the early stage, and once they appear, the symptoms of cognitive dysfunction and the pathological changes usually become severe and no therapeutic approaches can reverse progression. Therefore, early detection and intervention is important for reducing cognitive dysfunction in patients with CHP.

Past studies have shown that there is brain iron deposition in animals with CHP,[3] which is one of the major detrimental factors for cognitive function.[4,5] Brain iron deposition can be measured *in vivo* by non-invasive magnetic resonance imaging (MRI) based on the proton relaxation rate or magnetic field changes induced by the paramagnetic property of iron. Although many MRI sequences were proposed to represent brain iron concentration,[6] the phase signal is easily affected by the formation of the magnetic field distribution,[7] which would lead to inaccurate determination of brain iron level.

Recently, quantitative susceptibility mapping (QSM) has overcome these limitations because it is independent of field strength and object shape.[8] Additionally, QSM typically provides the highest sensitivity and specificity for detecting brain iron compared to other quantitative magnetic resonance (MR) methods[9–12] and has been applied to detect brain iron concentration in many brain diseases, such as Parkinson's disease,[13–18] Alzheimer's disease,[19] multiple sclerosis,[20–22] depression,[23] subcortical ischaemic vascular dementia (SIVD),[24] subcortical vascular mild cognitive impairment (MCI),[25] type 2 diabetes mellitus (T2DM),[26] military traumatic brain injury,[27] intracerebral haemorrhage,[28] pantothenate kinase-associated neurodegeneration,[29] vascular dementia (VaD), Alzheimer's dementia (AD),[30] and also in healthy older adults.[31]

The present study used the QSM method to investigate brain iron concentration in patients with CHP and neuropsychological tests to assess their cognitive function, and also analyse the correlation between brain iron concentration and cognitive impairment. The present findings indicate that brain iron deposition in specific areas may be responsible for cognitive impairment in CHP patients, and that QSM is a useful tool to determine brain iron, predicting cognitive impairment in CHP patients.

Materials and methods

Participants

A total of 40 participants, 23 patients with CHP and 17 age- and sex-matched healthy participants without CHP (control group), were enrolled in this study. All patients were admitted to the Department of Neurology, The Xinqiao Hospital of Third Military Medical University (Chongqing, China) during the period from March 2016 to December 2018. Patients compliant with the following criteria were enrolled into CHP group: (1) aged 50–80 years; (2) had risk factors of cerebrovascular diseases including hypertension, diabetes mellitus, hyperlipidaemia, etc.; and (3) suffered white matter lesions (WMLs) confirmed by hyperintensity on T2-weighted images and fluid-attenuated inversion recovery (FLAIR) MRI sequences. The participants in the control group, recruited from volunteers, met the following criteria: (1) aged 50–80 years; (2) no WMLs confirmed at brain MRI; (3) had complete neuropsychological scale and MRI data. The exclusion criteria for all participants included: (1) history of stroke, alcohol-related brain injury, Alzheimer's disease, Parkinson's disease, epilepsy, neurological or psychiatric disorders; (2) severe depression (Hamilton Depression Rating Scale $\geq$18), severe claustrophobia or other contraindications to MRI; (3) WMLs caused by other causes; (4) tumours; (5) autoimmune diseases; (6) haemochromatosis; and (7) alcohol abuse. All procedures performed in studies involving human participants were in accordance with the ethical standards of the institutional and/or national research committee and with the 1964 Helsinki declaration and its later amendments or comparable ethical standards. Informed consent was obtained from all participants with approval from the Medical Ethics Committee of Xinqiao Hospital of The Army (Third Military) Medical University. ClinicalTrials.gov Identifier: NCT02135783 (7 May 2014).

MRI

All the participants underwent whole-body 3-T MRI (Magnetom Trio, Siemens Healthcare, Erlangen, Germany) equipped with a 12-channel phased-array head coil. A high-resolution three-dimensional spoiled gradient-echo sequence was used to obtain susceptibility-weighted images (SWI) with the following parameters: 29 ms repetition time (TR), echo times (TEs) of 5, 10, 15, 20, 25, 30, and 35 ms; 15° flip angle, 2 mm section thickness, 256 × 256 mm field of view, and 512 × 512 matrix size. The T1-weighted images were obtained with the following parameters: 200 ms TR, 2.78 ms TE, 70° flip angle, 384 × 384 matrix, and 0.9 × 0.7 × 5 mm^3 voxel size, 30 sections. The FLAIR sequence was scanned using the following parameters: 9,000 ms TR, 93 ms TE, 2,500 ms inversion time (TI), 130° flip angle, 256 × 256 matrix, and 0.9 × 0.9 × 4.0 mm^3 voxel size, 40 sections.

Data processing

SMART (Susceptibility Mapping and Phase Artifacts Removal Toolbox, Detroit, MI, USA) and SPIN (Signal Processing in Nuclear magnetic resonance, MR Innovations, Detroit, MI, USA) software were used for SWI data processing and measurement.[32] According to the instructions for the SMART and reported methods,[33,34] the following steps were carried out: (1) high-pass filter of phase images, to remove most of the low spatial frequency phase; (2) K-space interpolation by zero filling the phase images in all three directions; (3) noise removal in the non-tissue region in the phase images using a complex thresholding approach on the

magnitude image, followed by the application of a skull stripping algorithm; (4) regularised inverse filter application to the Fourier transform of the high-pass filtered phase image.

Data analyses

Regions of interest (ROIs) were drawn manually on every section using SPIN software. The boundary of bilateral parietal cortex (PC), caudate nucleus (CN), putamen, globus pallidus (GP), thalamus, frontal white matter (FWM), hippocampus (HP), red nucleus (RN), and substantia nigra (SN) were drawn in the magnitude images as a mask, and the mask was then copied to the QSM image using SPIN software (Fig 1). The ROI in the FWM was circular and had an area of 100 pixels. Severity of WMLs was assessed on FLAIR images by two independent neurologists with >5 years of experience, as defined by the Age-related White Matter Change Score (0–3).[35] Participants with a score of 3 (diffuse involvement across the region) were excluded.[26,36]

Neuropsychological examinations

All participants underwent neuropsychological examinations by a qualified assessor, and the tests included Montreal Cognitive Assessment (MoCA), Mini Mental State Examination (MMSE), Hamilton Depression Scale (HAMD), Activities of Daily Living (ADL), Trail-Making Test parts A (TMT-A), Neuropsychiatric Inventory (NPI), Informant Questionnaire on Cognitive Decline in The Elderly (IQCODE), Digital Span Test-Forwards and Backwards (DST-Forwards and Backwards), Digit Symbol Coding (DSC) and verbal fluency. MCI was defined according to the criteria proposed by Petersen, including complaints of hypomnesis, MMSE score ≤24, and MoCA score <26.[26,37]

Statistical analysis

Statistical analyses were performed using SPSS software (version 18.0; SPSS, Chicago, IL, USA). Correlation analysis (Fig 2, and Electronic Supplementary Material Figs. S1 and S2) was conducted using linear regression analysis. Comparison of demographic data and neuropsychological test results between CHP patients and controls (Table 1) was performed using the *t*-test (for mean ± standard deviation) and chi-squared test (for proportions) and non-parametric test (Mann–Whitney *U*-test for median [quartile distance]). Comparison of MMSE characteristics (Table 2), MoCA characteristics (Table 3), and regional differences in

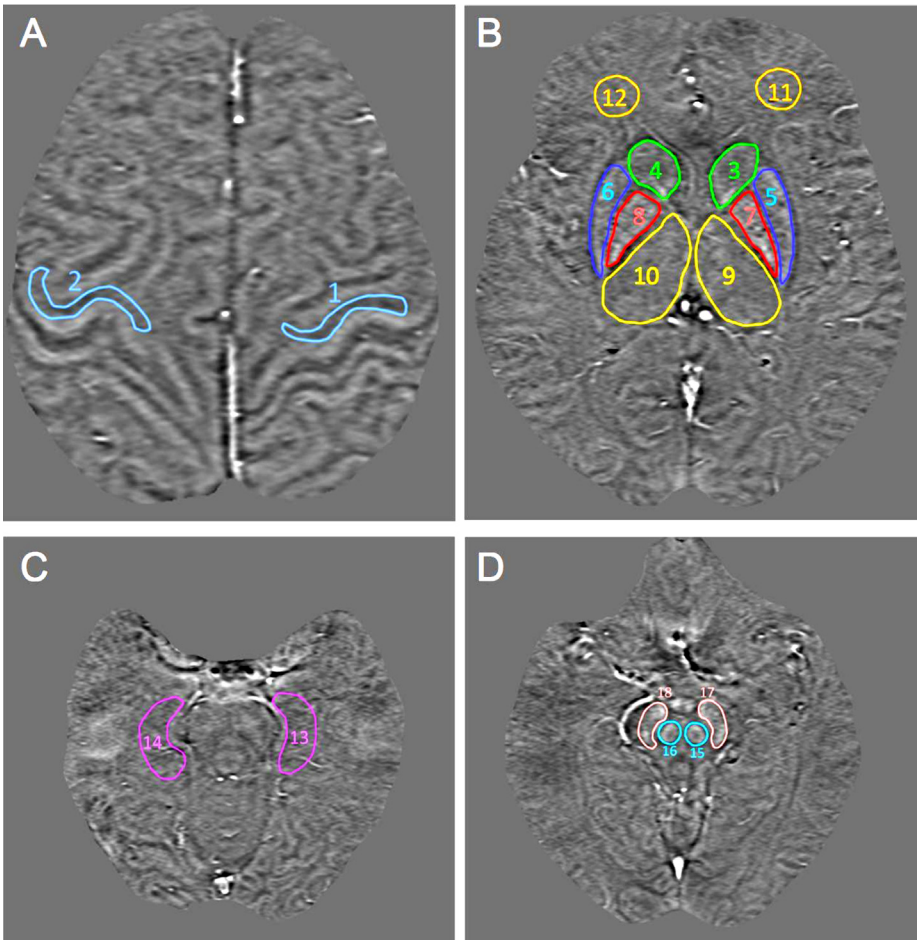

Figure 1 ROIs depicted on the QSM images.(a) 1, 2 = parietal cortex (PC, blue); (b) 3, 4 = caudate nucleus (CN, green); 5, 6 = putamen (putamen, blue); 7, 8 = globus pallidus (GP, red); 9, 10 = thalamus (thalamus, yellow); 11, 12 = frontal white matter (FWM, orange); (c) 13, 14 = hippocampus (HP, purple); (d) 15, 16 = red nucleus (RN, blue); and 17, 18 = substantia nigra (SN, pink).

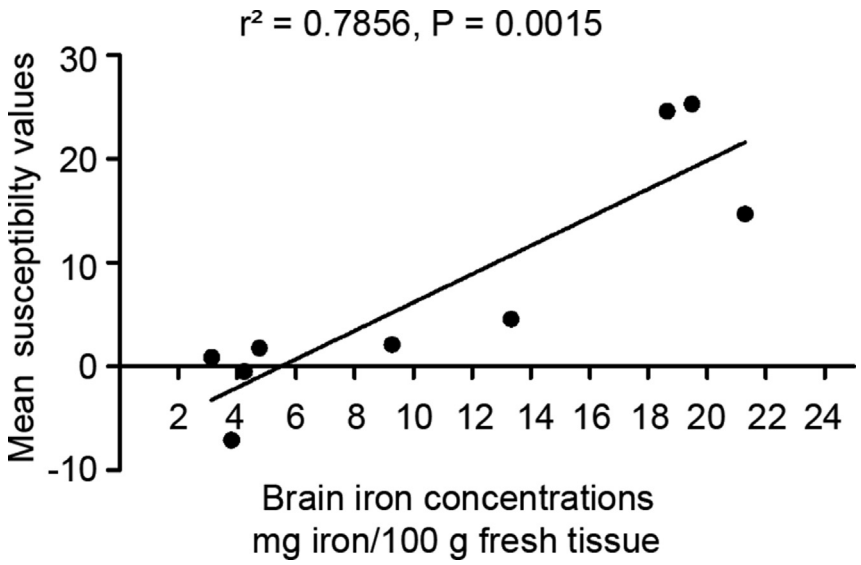

Figure 2 Correlation analysis of the relationship between brain susceptibility values of the 17 controls and iron concentrations (9.28, 13.32, 21.30, 4.76, 4.24, 3.13, 19.48, 18.64 and 3.81 mg per 100 g of wet weight) in the corresponding sub-regions of post-mortem brain in healthy adults reported by Hallgren & Sourander ($r^2 = 0.7856$, p=0.0015).

Table 1
Comparison of demographic data and neuropsychological test results between chronic cerebral hypoperfusion (CHP) patients and controls.

Characteristics	CHP patients (n=23)	Control participants (n=17)	p-Value
Age (years)	66.3 ± 6.3	59.5 ± 5.2	0.275
Sex (male, %)	52.2% (12/23)	47.1% (8/17)	0.925
Education (years)	7.9 ± 2.5	10.6 ± 3.5	0.181
MoCA/30	18.2 ± 5.9	22.9 ± 5.4	0.014
MMSE/30	24 ± 4.2	28 ± 2.9	0.002
HAMD	2.4 ± 2.4	3.5 ± 2.7	0.338
ADL/20-80	20 (1)	20 (1)	0.103[a]
TMT-A	98.8 ± 33.5	64.2 ± 23.5	0.177
NPI	0 (0)	0 (2)	0.799[a]
IQCODE	3.2 (0.4)	3.4 (0.3)	0.011[a]
DST-Forwards	6.9 ± 1.8	7.5 ± 1.4	0.325
DST-Backwards	3.8 ± 1.1	4.4 ± 0.8	0.071
DSC	22.5 ± 11.6	37.3 ± 13	0.473
Verbal fluency	13.5 ± 5.7	17 ± 4	0.037

Data were expressed as the mean ± standard deviation, proportion, and median (quartile distance).
MoCA, Montreal Cognitive Assessment; MMSE, Mini-Mental State Examination; HAMD, Hamilton Depression Scale; ADL, Activities of Daily Living; TMT-A, Trail-Making Test parts A; NPI, Neuropsychiatric Inventory; IQCODE, Informant Questionnaire on Cognitive Decline in The Elderly; DST-Forwards, Digital Span Test-Forwards; DST-Backwards, Digital Span Test-Backwards, DSC, Digit Symbol Coding.
[a] Data were not normally distributed (non-parametric tests).

Table 2
Comparison of Mini-Mental State Examination (MMSE) characteristics between chronic cerebral hypoperfusion (CHP) patients and control.

Characteristics	CHP patients (n=23)	Control participants (n=17)	p-Value
Time orientation/5	4.3 ± 0.9	4.9 ± 0.2	0.007
Place orientation/5	5 ± 0	4.9 ± 0.2	0.239
Immediate memory/3	2.7 ± 0.8	3 ± 0	0.102
Attention and calculation/5	3 ± 1.1	4.6 ± 1.2	0.001
Short term memory/3	1.7 ± 0.8	2.4 ± 0.9	0.027
Naming/2	2 ± 0	2 ± 0	1.000
Verbal comprehension/1	0.6 ± 0.5	0.9 ± 0.3	0.070
Reading comprehension/1	0.8 ± 0.4	0.9 ± 0.2	0.191
Language comprehension/3	2.4 ± 1	2.8 ± 0.6	0.194
Sentence speaking and writing/1	0.8 ± 0.4	0.9 ± 0.3	0.460
Paint/1	0.8 ± 0.4	0.9 ± 0.2	0.191

Data were expressed as the mean ± standard deviation.

mean susceptibility values (Tables 4 and 5) were conducted using the non-parametric test (Mann–Whitney U-test). A probability value of <0.05 was taken to indicate statistical significance.

Results

All participants, who met all of the inclusion and none of the exclusion criteria, were included. The demographic data and neuropsychological test results of the CHP group and control group are listed in Table 1. No significant difference was found between the two groups in terms of age, sex, and education level ($p>0.05$), while scores of MMSE, MoCA, ADL, and verbal fluency tests were significantly lower in the CHP group ($p<0.05$). Further respective comparisons of each item in the MMSE and MoCA showed only time orientation, short-term memory, attention, and calculation in MMSE, and visuoexecutive, attention, language, and recall in MoCA, were significantly different between the two groups ($p<0.05$; Tables 2 and 3).

The mean susceptibility values (ppb) of the right and left CN, putamen, GP, thalamus, FWM, HP, RN, SN, and PC subregions in the controls were 2.13, 4.59, 14.71, 1.78, −0.47, 0.87, 25.33, 24.61 and −7.08, respectively. There is a close positive correlation ($r^2 = 0.7856$, p=0.0015) between SWI mean susceptibility values and the published regional real iron concentrations as reported by Hallgren & Sourander[38] (Fig 2).

Table 3
Comparison of Montreal Cognitive Assessment (MoCA) characteristics between chronic cerebral hypoperfusion (CHP) patients and controls.

Characteristics	CHP patients (n=23)	Control participants (n=17)	p-Value
Visuoexecutive/5	4 (2)	3 (2)	0.033[a]
Naming/3	2.5 ± 1	2.5 ± 1.1	0.971
Attention/6	4.3 ± 1.3	5.5 ± 0.8	0.001
Language/3	1 (2)	1 (3)	0.038[a]
Abstraction/2	1.2 ± 0.9	1.3 ± 0.8	0.749
Recall/5	1.2 ± 1.2	2.2 ± 1.4	0.020
Orientation/6	4.5 ± 2.4	5.4 ± 1.6	0.202

Data were expressed as the mean ± standard deviation.
[a] Data were not normally distributed (non-parametric tests).

Compared with the controls, CHP patients exhibited a significant increase in mean susceptibility values in the bilateral HP and SN (p<0.05). No significant differences in mean susceptibility values were found in the bilateral PC, CN, GP, thalamus, FWM and RN between CHP and control groups (p>0.05; Table 4). Close correlations were found in CHP patients between the mean susceptibility values of the bilateral HP and MMSE and MoCA scores (left: r^2 = 0.3425, p=0.0034, right: r^2 = 0.3491, p=0.0030 for MMSE; left: r^2 = 0.1888, p=0.0383, right: r^2 = 0.4386, p=0.0006 for MoCA), left putamen and MMSE and MoCA scores (r^2 = 0.3796, p=0.0017; r^2 = 0.2486, p=0.0155, respectively; Electronic Supplementary Material Figs. S1 and S2).

No significant differences in mean susceptibility values were found in the bilateral PC, CN, GP, thalamus, FWM, and RN between CHP and control groups (p>0.05; Table 4). Close correlations were found in the CHP patients between mean susceptibility values of the bilateral HP and MMSE and MoCA scores (left: r^2 = 0.3425, p=0.0034, right: r^2 = 0.3491, p=0.0030 for MMSE; left: r^2 = 0.1888, p=0.0383, right: r^2 = 0.4386, p=0.0006 for MoCA), left putamen and MMSE and MoCA scores (r^2 = 0.3796, p=0.0017; r^2 = 0.2486, p=0.0155, respectively; Electronic Supplementary Material Figs. S1 and S2).

Additionally, depending on the scores of global cognitive functioning, the CHP patients were subdivided into an MCI group (MMSE score <24 and MoCA score <26, eight cases) and a normal cognition group (MMSE score ≥ 24 and MoCA score ≥ 26, 15 cases). Compared with the normal cognition group, the MCI group also exhibited significantly higher mean susceptibility values in the left putamen and bilateral HP (p<0.05; Table 5).

Table 4
Regional differences of mean susceptibility values between chronic cerebral hypoperfusion (CHP) patients and controls.

ROI	CHP (n=23)	NC (n=17)	Z-value	p-Value
Left PC	-8.99 (3.33)	-6.86 (6.88)	-0.81	0.420
Right PC	-9.07 (5.24)	-6.01 (5.50)	-1.82	0.069
Left CN	0.27 (8.76)	6.47 (14.26)	-0.42	0.672
Right CN	0.79 (11.18)	5.94 (12.67)	-0.37	0.712
Left putamen	4.51 (4.64)	7.48 (10.41)	-1.82	0.069
Right putamen	5.73 (4.18)	7.71 (6.61)	-1.90	0.057
Left GP	12.37 (11.56)	9.78 (12.38)	-1.16	0.245
Right GP	12.01 (4.36)	11.36 (14.99)	-1.60	0.109
Left thalamus	1.77 (2.47)	2.74 (2.70)	-0.59	0.556
Right thalamus	1.33 (2.35)	2.44 (2.70)	-0.62	0.538
Left FWM	0.33 (6.86)	0.65 (4.23)	-0.29	0.774
Right FWM	1.41 (5.01)	0.41 (3.63)	-0.23	0.816
Left HP	2.25 (6.42)	4.89 (3.18)	-3.05	0.002
Right HP	1.24 (4.58)	2.97 (2.40)	-3.52	0.000
Left RN	25.73 (10.58)	21.17 (14.99)	-1.22	0.223
Right RN	20.68 (20.90)	23.10 (14.70)	-0.45	0.652
Left SN	29.14 (16.26)	29.73 (9.94)	-2.15	0.032
Right SN	24.07 (17.15)	33.75 (11.67)	-3.57	0.000

Data were expressed as the median (quartile distance).
PC, parietal cortex; CN, caudate nucleus; putamen, putamen; GP, globus pallidus; thalamus, thalamus; FWM, frontal white matter; HP, hippocampus; RN, red nucleus; SN, substantia nigra.

Table 5
Regional differences of mean susceptibility values between chronic cerebral hypoperfusion (CHP) patients with or without mild cognitive impairment (MCI).

ROI	Normal (n=15)	MCI (n=8)	Z-value	p-Value
Left PC	-7.03 (6.98)	-8.74 (7.88)	-1.16	0.245
Right PC	-6.01 (3.68)	-6.93 (8.32)	-0.07	0.949
Left CN	2.16 (14.37)	6.17 (9.30)	-0.52	0.606
Right CN	4.09 (12.19)	4.92 (14.61)	-0.55	0.583
Left putamen	5.74 (6.86)	13.09 (9.79)	-2.26	0.024
Right putamen	6.71 (5.83)	9.12 (7.45)	-0.78	0.439
Left GP	9.78 (7.81)	13.81 (15.85)	-0.58	0.561
Right GP	10.27 (5.36)	11.69 (18.22)	-0.90	0.366
Left thalamus	1.68 (3.34)	2.47 (2.63)	-0.71	0.478
Right thalamus	1.99 (2.25)	2.74 (2.85)	-1.36	0.175
Left FWM	0.33 (2.82)	-0.06 (6.13)	0.00	1.000
Right FWM	1.68 (5.38)	0.39 (5.13)	-0.52	0.606
Left HP	3.29 (2.99)	5.86 (1.73)	-3.10	0.002
Right HP	2.73 (1.74)	5.19 (2.96)	-2.71	0.007
Left RN	21.04 (15.95)	21.05 (9.78)	-0.32	0.747
Right RN	26.73 (21.48)	21.37 (10.57)	-0.52	0.606
Left SN	29.73 (6.04)	34.15 (20.84)	-0.97	0.333
Right SN	32.01 (7.63)	39.13 (17.76)	-1.87	0.061

Data are expressed as the median (quartile distance).
PC, parietal cortex; CN, caudate nucleus; putamen, putamen; GP, globus pallidus; thalamus, thalamus; FWM, frontal white matter; HP, hippocampus; RN, red nucleus; SN, substantia nigra.

Discussion

Because invasive measurement of iron levels in the human brain is not feasible, several MRI methods, particularly QSM, have been used to detect iron in the brain *in vivo*,[12,13] as well as to assess brain iron deposits associated with normal aging and several brain diseases.[39–42]

Using QSM, Li *et al.*[14] investigated the iron levels of different subcortical and limbic structures of Parkinson's disease patients with dementia (PDD) and without dementia and provided further evidence for iron accumulation in the limbic structures of PDD and Parkinson's disease patients and its correlation with cognitive performance. Shahmaei *et al.*[17] reported that using QSM in RN, SN, and GP nuclei can help with diagnosis and staging of patients with Parkinson's disease. A study by Uchida *et al.*[18] suggested that cognitive impairment in Parkinson's disease is associated with cerebral iron burden and highlighted the potential of quantitative susceptibility mapping as an auxiliary biomarker for early evaluation of cognitive decline in

patients with Parkinson's disease. Using a two-region of interest analysis on QSM, Sethi *et al.*[16] showed that abnormal iron occurs in idiopathic Parkinson's disease patients in the SN with greater volumes when compared to healthy controls. Chen *et al.*[15] also demonstrated that Parkinson's disease is closely related to iron deposition in the SN by using QSM. In addition, Gong *et al.*[19] showed that QSM can be used to longitudinally monitor beta amyloid accumulation and accompanying iron deposition *in vivo* in a transgenic mouse model of Alzheimer's disease. QSM values reported by Zivadinov *et al.*[21] suggest that altered deep grey matter iron is associated with the evolution of multiple sclerosis and disability accrual, independent of tissue atrophy. These findings provide neuroimaging-based evidence for the association of increased brain iron with neurodegenerative disorders.

QSM has also been used to measure iron levels in the brain in other diseases. Yao *et al.*[23] provided QSM evidence that cerebral iron deposition may be related to depression. Yang *et al.*[26] reported that T2DM is associated with cerebral iron deposition and suggested that QSM may be a useful tool for the detection and assessment of cognitive impairment in T2DM patients. Sun *et al.*[25] found that cerebral iron levels are correlated with cognitive impairment severity in subcortical vascular MCI participants, implying that cerebral iron deposition could be a biomarker for cognition in clinic. Comparison of the pattern and presence of brain iron accumulation with VaD and AD using QSM showed that increases in iron deposition in the putamen and caudate nuclei are not associated with age or severity of cognitive impairment in VaD and AD patients.[30]

In spite of the above, up to now, QSM has not been used to investigate brain iron deposition and its relationship with cognitive impairment in patients with CHP. Thus, the present study examined the presence of iron accumulation in patients with CHP and the effect of iron on cognition. A close correlation was found between the regional brain susceptibility values in different brain regions of the normal controls and the real brain iron concentrations measured by chemical colorimetry in 81 normal autopsy brains by Hallgren & Sourander.[38] This indicated that the present QSM methods are reliable for the non-invasive estimation of regional brain iron deposition.

The present study demonstrated that CHP patients had poorer cognitive function compared with the age- and sex-matched control participants, as evaluated by MMSE, MoCA, ADL, and verbal fluency tests. In addition, more iron was deposited in both sides of putamen, HP, and SN in CHP patients, and the susceptibility of bilateral HP and left putamen was closely correlated with their cognitive impairment; however, the asymmetrical findings in the putamen may be related to disease specificity and lower sample size; therefore, a larger sample size should be used to verify this conclusion in future studies. Furthermore, CHP patients with MCI had higher susceptibility values (or brain iron deposition) of bilateral putamen, HP, and SN as compared with CHP patients without MCI (normal cognition). Previous studies also showed that increased susceptibility values within the HP and putamen were correlated with T2DM-related cognitive impairment[26] and subcortical vascular mild cognitive impairment.[25] In Sun *et al.*,[25] in the putamen (right (left) hemisphere) susceptibility values of 74 (72) ppb/61 (71) ppb in MCI patients/controls were reported; differences were only significant for the right putamen. In this study, differences between CHP patients with and without MCI were only significant for the left putamen with 6 ppb/13 ppb in patients without/with MCI. In the HP (both hemispheres), Sun *et al.* found susceptibility values of 52 ppb/38 ppb in MCI patients/controls compared to 5–6 ppb/3 ppb for patients with/without MCI in this study. Together, these results indicated that cognitive impairment is common in CHP patients even though they have yet to show any other neurological symptoms, and also suggests that iron deposition in specific brain areas is responsible for the cognitive impairment in CHP patients.

The putamen, HP, and SN are important brain structures for the execution of normal brain functions, such as memory, emotion, reward, movement, learning, and addiction. Therefore, injury of these areas would result in cognitive impairment.[43,44] Iron deposition in brain tissue may lead to neuronal damage, likely through increasing free radicals, promoting lipid peroxidation, and ultimately, causing oxidative stress injury.[45,46] Hence, it is reasonable to believe that iron deposition in the specific brain areas observed in this study is an important causative factor for the cognitive impairment observed in CHP patients.

To the authors' knowledge, the current study is the first to explore the relationship between brain iron deposition and cognitive impairment in patients with CHP using the QSM method. The present findings show that brain iron deposition is positively correlated with cognitive impairment in patients with CHP, indicating that brain iron accumulation in specific brain areas, such as the HP and putamen, may contribute to cognitive impairment. The data also demonstrate that the QSM method is a useful tool for determining iron levels in the brain, predicting cognitive impairment in patients with CHP and also other neurodegenerative disorders; however, the sample size is relatively small in the present study. Therefore, prospective studies with larger sample sizes should be conducted in the future to validate the conclusions made here.

Conflict of interest

The authors declare no conflict of interest.

Acknowledgements

This study was supported by the Natural Science Foundation of China (81771136 to Y.L. and 31571195 to Z.-M.Q.).

Appendix A. Supplementary data

Supplementary data to this article can be found online at https://doi.org/10.1016/j.crad.2023.02.020.

References

1. Choi BR, Kim DH, Back DB, *et al*. Characterization of white matter injury in a rat model of chronic cerebral hypoperfusion. *Stroke* 2016;**47**(2):542–7.
2. Ruitenberg A, den Heijer T, Bakker SL, *et al*. Cerebral hypoperfusion and clinical onset of dementia: the Rotterdam Study. *Ann Neurol* 2005;**57**(6):789–94.
3. Li Y, He Y, Guan Q, *et al*. Disrupted iron metabolism and ensuing oxidative stress may mediate cognitive dysfunction induced by chronic cerebral hypoperfusion. *Biol Trace Elem Res* 2012;**150**(1–3):242–8.
4. Ghadery C, Pirpamer L, Hofer E, *et al*. R2* mapping for brain iron: associations with cognition in normal aging. *Neurobiol Aging* 2015;**36**(2):925–32.
5. Smith MA, Zhu X, Tabaton M, *et al*. Increased iron and free radical generation in preclinical Alzheimer disease and mild cognitive impairment. *J Alzheimers Dis* 2010;**19**(1):363–72.
6. Aquino D, Bizzi A, Grisoli M, *et al*. Age-related iron deposition in the basal ganglia: quantitative analysis in healthy participants. *Radiology* 2009;**252**(1):165–72.
7. Schweser F, Deistung A, Lehr BW, *et al*. Quantitative imaging of intrinsic magnetic tissue properties using MRI signal phase: an approach to *in vivo* brain iron metabolism? *Neuroimage* 2011;**54**(4):2789–807.
8. Wharton S, Bowtell R. Whole-brain susceptibility mapping at high field: a comparison of multiple- and single-orientation methods. *Neuroimage* 2010;**53**(2):515–25.
9. Liu C, Li W, Tong KA, *et al*. Susceptibility-weighted imaging and quantitative susceptibility mapping in the brain. *J Magn Reson Imaging* 2015;**42**(1):23–41.
10. Wang Y, Liu T. Quantitative susceptibility mapping (QSM): decoding MRI data for a tissue magnetic biomarker. *Magn Reson Med* 2015;**73**(1):82–101.
11. Wang Y, Spincemaille P, Liu Z, *et al*. Clinical quantitative susceptibility mapping (QSM): biometal imaging and its emerging roles in patient care. *J Magn Reson Imaging* 2017;**46**(4):951–71.
12. De Barros A, Arribarat G, Combis J, *et al*. Matching *ex vivo* MRI with iron histology: pearls and pitfalls. *Front Neuroanat* 2019;**13**:68.
13. Langkammer C, Pirpamer L, Seiler S, *et al*. Quantitative susceptibility mapping in Parkinson's disease. *PLoS One* 2016 6;**11**(9):e0162460.
14. Li Dthalamus, Hui ES, Chan Q, *et al*. Quantitative susceptibility mapping as an indicator of subcortical and limbic iron abnormality in Parkinson's disease with dementia. *Neuroimage Clin* 2018;**20**:365–73.
15. Chen Q, Chen Y, Zhang Y, *et al*. Iron deposition in Parkinson's disease by quantitative susceptibility mapping. *BMC Neurosci* 2019;**20**(1):23.
16. Sethi SK, Kisch SJ, Ghassaban K, *et al*. Iron quantification in Parkinson's disease using an age-based threshold on susceptibility maps: the advantage of local versus entire structure iron content measurements. *Magn Reson Imaging* 2019;**55**:145–52.
17. Shahmaei V, Faeghi F, Mohammdbeigi A, *et al*. Evaluation of iron deposition in brain basal ganglia of patients with Parkinson's disease using quantitative susceptibility mapping. *Eur J Radiol Open* 2019;**6**:169–74.
18. Uchida Y, Kan H, Sakurai K, *et al*. Voxel-based quantitative susceptibility mapping in Parkinson's disease with mild cognitive impairment. *Mov Disord* 2019;**34**(8):1164–73.
19. Gong NJ, Dibb R, Bulk M, *et al*. Imaging beta amyloid aggregation and iron accumulation in Alzheimer's disease using quantitative susceptibility mapping MRI. *Neuroimage* 2019;**191**:176–85.
20. Zhang Y, Gauthier SA, Gupta A, *et al*. Longitudinal change in magnetic susceptibility of new enhanced multiple sclerosis (MS) lesions measured on serial quantitative susceptibility mapping (QSM). *J Magn Reson Imaging* 2016;**44**(2):426–32.
21. Zivadinov R, Tavazzi E, Bergsland N, *et al*. Brain iron at quantitative MRI is associated with disability in multiple sclerosis. *Radiology* 2018;**289**(2):487–96.
22. Zhang S, Nguyen TD, Hurtado Rúa SM, *et al*. Quantitative susceptibility mapping of time-dependent susceptibility changes in multiple sclerosis lesions. *AJNR Am J Neuroradiol* 2019;**40**(6):987–93.
23. Yao S, Zhong Y, Xu Y, *et al*. Quantitative susceptibility mapping reveals an association between brain iron load and depression severity. *Front Hum Neurosci* 2017;**11**:442.
24. Liu C, Li C, Yang J, *et al*. Characterizing brain iron deposition in subcortical ischaemic vascular dementia using susceptibility-weighted imaging: an *in vivo* MR study. *Behav Brain Res* 2015;**288**:33–8.
25. Sun Y, Ge X, Han X, *et al*. Characterizing brain iron deposition in patients with subcortical vascular mild cognitive impairment using quantitative susceptibility mapping: a potential biomarker. *Front Aging Neurosci* 2017;**9**:81.
26. Yang Q, Zhou L, Liu C, *et al*. Brain iron deposition in type 2 diabetes mellitus with and without mild cognitive impairment—an *in vivo* susceptibility mapping study. *Brain Imaging Behav* 2018;**12**(5):1479–87.
27. Liu W, Yeh PH, Nathan DE, *et al*. Assessment of brain venous structure in military traumatic brain injury patients using susceptibility weighted imaging and quantitative susceptibility mapping. *J Neurotrauma* 2019;**36**(14):2213–21.
28. De A, Sun H, Emery DJ, *et al*. Rapid quantitative susceptibility mapping of intracerebral haemorrhage. *J Magn Reson Imaging* 2020;**51**(3):712–8.
29. Zeng J, Xing W, Liao W, *et al*. Magnetic resonance imaging, susceptibility weighted imaging and quantitative susceptibility mapping findings of pantothenate kinase-associated neurodegeneration. *J Clin Neurosci* 2019;**59**:20–8.
30. Moon Y, Han SH, Moon WJ. Patterns of brain iron accumulation in vascular dementia and Alzheimer's dementia using quantitative susceptibility mapping imaging. *J Alzheimers Dis* 2016;**51**(3):737–45.
31. van Bergen JMG, Li X, Quevenco FC, *et al*. Simultaneous quantitative susceptibility mapping and flutemetamol-PET suggests local correlation of iron and β-amyloid as an indicator of cognitive performance at high age. *Neuroimage* 2018;**174**:308–16.
32. Pandian DS, Ciulla C, Haacke EM, *et al*. Complex threshold method for identifying pixels that contain predominantly noise in magnetic resonance images. *J Magn Reson Imaging* 2008;**28**(3):727–35.
33. Haacke EM, Tang J, Neelavalli J, *et al*. Susceptibility mapping as a means to visualize veins and quantify oxygen saturation. *J Magn Reson Imaging* 2010;**32**(3):663–76.
34. Haacke EM, Liu S, Buch S, *et al*. Quantitative susceptibility mapping: current status and future directions. *Magn Reson Imaging* 2015;**33**(1):1–25.
35. Wahlund LO, Barkhof F, Fazekas F, *et al*. European Task Force on Age-Related White Matter Changes. A new rating scale for age-related white matter changes applicable to MRI and CT. *Stroke* 2001;**32**(6):1318–22.
36. Cui Y, Jiao Y, Chen HJ, *et al*. Aberrant functional connectivity of default-mode network in type 2 diabetes patients. *Eur Radiol* 2015;**25**(11):3238–46.
37. Petersen RC. Mild cognitive impairment as a diagnostic entity. *J Intern Med* 2004;**256**(3):183–94.
38. Hallgren B, Sourander P. The effect of age on the non-haemin iron in the human brain. *J Neurochem* 1958;**3**(1):41–51.
39. Achiriloaie AF, Kido D, Wycliffe D, *et al*. White matter micro-susceptibility changes in patients with hepatic encephalopathy. *J Radiol Case Rep* 2011;**5**(8):1–7.
40. Langkammer C, Schweser F, Krebs N, *et al*. Quantitative susceptibility mapping (QSM) as a means to measure brain iron? A post mortem validation study. *Neuroimage* 2012;**62**(3):1593–9.
41. Bilgic B, Pfefferbaum A, Rohlfing T, *et al*. MRI estimates of brain iron concentration in normal aging using quantitative susceptibility mapping. *Neuroimage* 2012;**59**(3):2625–35.
42. Schweser F, Sommer K, Deistung A, *et al*. Quantitative susceptibility mapping for investigating subtle susceptibility variations in the human brain. *Neuroimage* 2012;**62**(3):2083–100.
43. Bastos-Leite AJ, van der Flier WM, van Straaten EC, *et al*. The contribution of medial temporal lobe atrophy and vascular pathology to cognitive impairment in vascular dementia. *Stroke* 2007;**38**(12):3182–5.
44. Kantarci K, Avula R, Senjem ML, *et al*. Dementia with Lewy bodies and Alzheimer disease: neurodegenerative patterns characterized by DTI. *Neurology* 2010;**74**(22):1814–21.
45. Ke Y, Ming Qian Z. Iron misregulation in the brain: a primary cause of neurodegenerative disorders. *Lancet Neurol* 2003;**2**(4):246–53.
46. Ke Y, Qian ZM. Brain iron metabolism: neurobiology and neurochemistry. *Prog Neurobiol* 2007;**83**(3):149–73.